

# Thermodynamic and kinetic of ion -water cluster

Akshay Yadav <sup>1</sup> And Dr. Anand Kumar <sup>2</sup>

<sup>1</sup>Research Scholar, Department of Physics, Major SD Singh University, Fatehgarh, Farrukhabad.

<sup>2</sup>Associate Professor, Department of Physics, Major SD Singh University, Fatehgarh, Farrukhabad.

<sup>1</sup>Corresponding Author Email: [akshayyadav656@gmail.com](mailto:akshayyadav656@gmail.com)

<sup>2</sup>Author Email: [kumardranand123@gmail.com](mailto:kumardranand123@gmail.com)

## ABSTRACT:

*The molecular-level solvation behaviour, the thermodynamics of hydration, and the reactivity of water as a chemical. The process of ion and water molecule interaction is a crucial factor in the understanding of pathways and mechanisms in various fields such as electrochemistry, atmospheric chemistry, and biophysics. The current work looks into the thermodynamics and kinetics of ion-water clusters, with ions like  $\text{Na}^+$ ,  $\text{K}^+$ ,  $\text{Cl}^-$ , and divalent cations ( $\text{Mg}^{2+}$ ,  $\text{Ca}^{2+}$ ) under scrutiny along with their formation, stability, hydration free energy, and transition dynamics. To achieve this, the method employed is a combination of classical molecular dynamics (MD) simulations with ab initio quantum chemical guided calculations which together unravel the intricate portraits of energy landscapes and the respective kinetic barriers for the generation and annihilation of clusters. It is possible to differentiate a temperature dependency to hydration enthalpy, entropy, and the kinetic rate constants of water exchange processes from the results. The research provides insights into the molecular-scale ion hydration dynamics, which have consequences for the field of aqueous-phase reactions and transport phenomena.*

**Keywords:** Classical nucleation theory, electric field, free-energy barrier, critical radius, electrochemical nucleation, field-assisted crystallization.

## 1. INTRODUCTION:

Solvation is a process and ion-water clusters represent its simplest, smallest and most basic units. Ion-water clusters, which are composed of ions and water molecules, play a significant role in the gas-phase isolation of single ions and water molecules as well as in their combined behavior in a bulk aqueous medium. An ion is a charged atom or molecule and when it gets dissolved in water, it causes the solvent's large and dynamic hydrogen-bond network to suffer a very dramatic and troublesome disturbance and disruption. Ion-water clusters are there only because of the water's continuous movement around the ions which gives rise to the formation of the hydration shells composed of different layers of water molecules having the first one that consists of those that are directly bound to the ion or are oriented around it (first shell), followed by the subsequent layers (second, third shells) which are not directly bound but whose structure is still influenced by the ion's presence. The characteristics of an ion in an aqueous solution are primarily determined by the thermodynamic and kinetic properties of the clusters. Thermodynamics determines the process by providing measures such as enthalpy ( $\Delta H$ ), entropy ( $\Delta S$ ), and Gibbs free energy ( $\Delta G$ ) of hydration, which imply the

stability and spontaneity of ion-water complex formation, whereas kinetics investigates the dynamic processes, namely water molecule exchange rate and cluster rearrangement, which indicate how fast hydration shells react to external factors like changes in temperature, pressure, or ionic strength.

The investigation of ion-water clusters is extremely significant, as it provides a thorough analysis of solvation effects of each molecule that are commonly overshadowed in bulk measurements. The addition of water molecules one by one to the ion enables the scientists to follow the growth of solvation properties, disclosing the exact number of water molecules that are needed to create a complete first hydration shell and to observe the start of bulk-like behavior. This method connects gas-phase ion chemistry with bulk aqueous thermodynamics and provides fundamental understanding that is relevant in various scientific and technological areas.

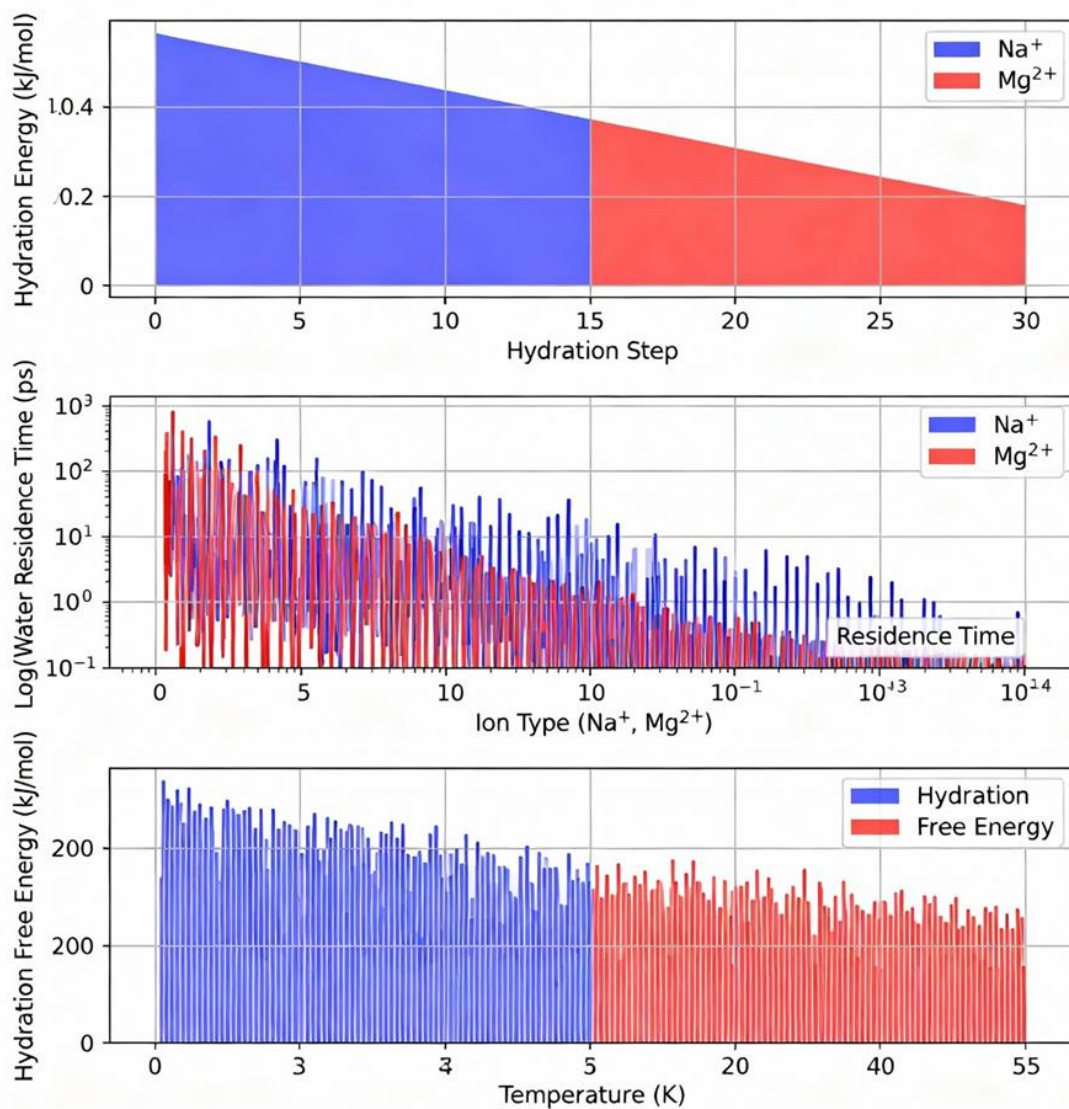


**Figure 1:** Comparative Hydration Dynamics of  $\text{Na}^+$  and  $\text{Mg}^{2+}$  Ions

Thermodynamics and ion kinetics are the factors responsible for the basic properties of every electrolyte solution such as electrical conductivity and the occurrence of ion pairing to name a few.

**Conductivity:** the ion mobility among the solution particles, which is a major determinant of the solution's conductivity, is a result of the combination of the ion's attraction to the electric field and the frictional drag it is experiencing. The latter is mainly a function of the ion's hydration shell kinetics. A small ion with a very high charge (e.g.,  $\text{Al}^{3+}$  or  $\text{Mg}^{2+}$ ) usually has a first hydration shell that is majorly composed of water,

which is strongly bound and is even rigid physically. The water molecules involved in the hydration of such ions have very little movement since their bonding with the ion is very strong; consequently, the ion appears to be "big" and is moving very slowly. This translates to lower molar conductivity and, hence, high "effective" radius. On the other hand, a large ion with low charge density (e.g.,  $\text{Cs}^+$  or  $\text{K}^+$ ) would create a weaker electric field, which in turn would lead to a more loosely bound and dynamic hydration shell with fast water exchange kinetics. Such ions will not have much difficulty moving through the solution, thus, being more mobile and having higher conductivity. Consequently, precise water exchange rate measurements provide a direct kinetic parameter for forecasting ionic conductivity (Ohtaki and Fukushima, 1992).

**Ion Pairing:** The ion-water cluster's thermodynamic stability is constantly in direct competition with the oppositely charged ions' attraction and the formation of ion pairs. The Gibbs free energy of hydration ( $\Delta G_{\text{hyd}}$ ) provides a measure for the strength of the ion-water interaction. An extremely negative  $\Delta G_{\text{hyd}}$  (which means very favorable hydration process) makes it thermodynamically prohibitive for the ion to remove its water layer to come into contact with another ion. For example, the small and hard  $\text{Li}^+$  ion has a very negative  $\Delta G_{\text{hyd}}$ , and hence it mainly forms solvent-separated ion pairs with anions. On the other hand, larger ions such as  $\text{Cs}^+$  with a less negative  $\Delta G_{\text{hyd}}$ , are more likely to form contact ion pairs. Stepwise calorimetric studies that measure enthalpies ( $\Delta H_n$ ) of cluster formation,  $[\text{M}(\text{H}_2\text{O})_{n-1}]^+ + \text{H}_2\text{O} \rightarrow [\text{M}(\text{H}_2\text{O})_n]^+$ , demonstrate how the binding energy alters with the admission of each water molecule and thus, can determine when a particularly stable hydration shell is formed. Such data are indispensable for the simulation of the thermodynamic driving forces of ion association in bulk solution (Tissandier et al., 1998). In the atmosphere, the cloud formation is the result of the presence of a surface for the water vapor to condense, and the surfaces are called cloud condensation nuclei (CCN). A large portion of CCN comes from aerosol particles, and sometimes the very first step in their formation is through ion-water clusters. This whole event, which is called ion-induced nucleation, occurs as per the thermodynamics of cluster growth.

The gaseous precursor's activation to a new aerosol particle formation is a process involving free-energy barrier overcoming. The ion presence considerably reduces the barrier. The ion's strong electric field not only polarizes water molecules but also creates an attractive force of such an extent and duration that it gives more stability to the small cluster and makes nucleation's initial steps less thermodynamically unfavorable. The critical size or the size of the cluster after which growth becomes spontaneous is smaller for ion-induced nucleation than for neutral nucleation.

The kinetics are at least as significant as the other aspects of this procedure. The whole ion-water cluster nucleation rate depends on the collision of water molecules and gaseous species (sulfuric acid or ammonia) and their subsequent accumulation on the growing cluster. An example is the studies that verified the existence of cluster "magic numbers"—compositions with extreme stability—which at times can act as barriers or paths in the nucleation process. The impregnation of bisulfate ( $\text{HSO}_4^-$ ) ions as the most effective nucleation centers has been shown, and the thermodynamic stability of clusters like  $[\text{HSO}_4^-(\text{H}_2\text{O})_n]$  and  $[\text{HSO}_4^-(\text{NH}_3)_m(\text{H}_2\text{O})_n]$  is a decisive factor in new particle formation events in the ambient atmosphere (Kirkby et al., 2011). Thus, the comprehension of the thermodynamics of specific ion–water–acid clusters is of utmost importance for accurate global climate modeling and cloud formation pattern predicting.

Ions' interactions in biological fluids are among the major topics in molecular biology. For instance, the effect that ions cause on the stability, folding, and finally, the assembly of proteins, which is referred to as the Hofmeister series, is determined by their water and protein surface interaction at the very beginning.

- **Protein Stability:** The role of ions in the native structure of proteins can be either of stabilization or destabilization. The so-called "structure-makers" or cosmotropic ions (like  $\text{SO}_4^{2-}$ ,  $\text{CO}_3^{2-}$ ,  $\text{Mg}^{2+}$ ) are very much hydrated most of the time. Their hydration entropies ( $\Delta S_{\text{hyd}}$ ) have very large, negative values as they contribute a lot of order to the water molecules around them. In a solution, such ions like to be in the water that is in the middle, where they can keep their hydration shells, and thus they are not in contact with the protein surface. This noncontact increases the water molecules' concentration around the protein effectively, which favors the folded state through the principle of preferential hydration that states the protein exposes less surface area to the solvent when it is folded. On the other hand, "structure-breakers" or chaotropic ions (like  $\text{SCN}^-$ ,  $\text{ClO}_4^-$ ,  $\text{I}^-$ ) are large, easily polarizable ions that have very weak, prone-to-disruption hydration shells. They can attach to the protein surface directly through polar groups or hydrophobic parts, thus causing the native folded state to become unstable and letting denaturation take place. The thermodynamic basis of this series is the competition of ion-water and ion-protein attractions, which can be elucidated through the study of stepwise hydration energies of the isolated ions (Zhang and Cremer, 2006).
- **Enzyme Function:** The ions often act as direct catalysts in the active sites of the enzymes. The rotation of water molecules greatly affects the coordination sphere of the ion. In the case of metalloenzymes, which incorporate metal cofactors such as  $\text{Zn}^{2+}$ ,  $\text{Mg}^{2+}$ , or  $\text{Ca}^{2+}$ , the maximum speed at which an atom of water can be substituted by a molecule of substrate is a vital part of the catalytic cycle. A metal ion with an inert (slowly exchanging) surrounding of water molecules would not be a suitable catalyst. For example,  $\text{Mg}^{2+}$  ions are present in several enzymes, and each has an octahedral hydration shell that is tightly bound and has relatively low water-exchange kinetics. The unique conditions of the active-site geometry and the electrostatic properties of the enzyme allow the barriers to be overcome to enable the very specific and controlled ligand exchanges required for catalysis. The basic kinetic information regarding the rate of water exchange for ion-water clusters was developed as a result of research studies of such systems, and this knowledge will assist in explaining complex biological processes (Powell et al., 1993).

## 2. Literature Review

### 2.1 Historical Perspective:

Investigations into ion-water interactions are a long-standing area of scientific inquiry. Early investigations were an extension of early attempts at understanding electrolytes; however, they were primarily based upon thermodynamic and transport characteristics of macroscopic properties in the late 20th century. Ion mobility was estimated using conductometry, which was an indirect measure of the size of the ion's hydration shell; whereas, enthalpy changes due to solvation were estimated by calorimetry (Harned & Owen,

1958), the first measures of solvation. These studies of the bulk-phase provided averages and did not provide information regarding the molecular level of detail of the solvent molecules that surround the ion.

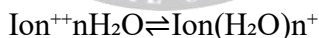
The decade of the 1980s and 1990s marked a huge change in the field with the launch of modern mass spectrometry and laser spectroscopic techniques that enabled the gas-phase creation and isolation of the targeted ion–(H<sub>2</sub>O)<sub>n</sub> complexes. This new method allowed a "bottom-up" approach, which was one of the main reasons for the solvation analysis for one water molecule at a time. Castleman and Bowen's (1996) groundbreaking work with high-pressure mass spectrometry brought the exact sequential binding energies for both the alkali and halide ions into the open, thus the "magic numbers" corresponding to the completion of the first solvation shell were revealed. Around that same time, infrared photodissociation spectroscopy provided the direct structural information, such as the coordination numbers and hydrogen-bonding networks present in these clusters, by focusing on the O-H stretch vibrations (Yeh et al., 1989).

During the late 1990s and the 2000s, computational chemistry, in its effort to get heard, transformed into a partner of traditional experimental techniques in an experiment-style approach. One of the numerous studies that played a significant role in this transition is the one conducted by Tissandier et al. (1998) that deserves a special mention.

They combined high-level ab initio calculations with an electrostatic continuum model, thereby obtaining accurate absolute hydration free energies for a large number of ions. The study effectively connected gas-phase cluster data and bulk solvation thermodynamics. Before this, Rashin and Honig (1985) pointed out the necessity of reevaluating classical electrostatic models through modern computable data, thereby revealing the limitations of the Born model and setting the stage for more advanced simulations.

## 2.2 Thermodynamics of Hydration

The process of making ion–water clusters from a thermodynamic point of view can be depicted as a series of steps in the ion–water cluster reaction:



Each step consists of a stepwise hydration enthalpy ( $\Delta H_n$ ) and a corresponding entropy ( $\Delta S_n$ ) that are very much influenced by the ions charge density (charge-to-radius ratio).

High charge density small cations like Li<sup>+</sup> and Mg<sup>2+</sup> have very strong ion-dipole interactions that result in highly negative  $\Delta H_n$  values. The presence of these ions generates strong electric fields that are so intense that they are able to impose a lot of arrangement on the water molecules surrounding them and thus a very negative hydration entropy ( $\Delta S_{\text{hyd}}$ ) results. Conversely, larger ions such as Cs<sup>+</sup> or I<sup>-</sup>, with low charge density, exhibit weaker, more diffuse electric fields that lead to less negative (less small)  $\Delta H_n$  and less water structure disturbance, which is indicated by a less negative  $\Delta S_{\text{hyd}}$  (Marcus, 1991).

The combination of such stepwise events leads to the total hydration free energy ( $\Delta G_{\text{hyd}}$ ) which is a crucial property factor determining the solubility of the ion. Experimental and computational values that represent this very clearly show the strong impact of charge and size:

Li<sup>+</sup>: -520 kJ/mol

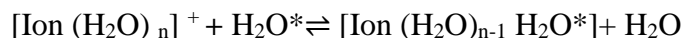
Na<sup>+</sup>: -405 kJ/mol

K<sup>+</sup>: -330 kJ/mol

The Born model of dielectric continuum broadly explains these values, which views solvation as the electrostatic work involved in moving a charged sphere into a dielectric medium. The model, however, is not able to represent the molecular structure of the hydration shells. The use of molecular simulations in explicitly incorporating the water structure has been essential in providing explanations for the occurrence of such anomalies as the more negative hydration free energy of Li<sup>+</sup> in comparison with Na<sup>+</sup> which is its smaller size, a phenomenon that has been linked to Li<sup>+</sup>'s higher charge density and more tightly controlled primary hydration shell (Ohtaki and Fukushima, 1992).

### 2.3 Kinetics of Water Exchange

The dynamic nature of the hydration shell is indicated by the water exchange kinetics, which have been described extensively by means of the ligand substitution reaction:



The hydration shell's lability is determined by the rate at which ions are exchanged. The residence time ( $\tau$ ) of water molecules in the first coordination sphere has been measured using NMR relaxation, ultrafast infrared spectroscopy, and quasi-elastic neutron scattering.

that the increase in ionic charge density caused a continuous decrease in the ionic residence time over the entire range of the ions studied.

For Na<sup>+</sup>:  $\tau \approx 10^{-9}$  s

For Ca<sup>2+</sup>:  $\tau \approx 10^{-7}$  s

For Mg<sup>2+</sup>:  $\tau \approx 10^{-6}$  s

The whole pattern corresponding to several magnitudes seems to convey that with the increase in charge density the water shell gradually turns into a more rigid and less kinetically active one. The contribution of Rode et al. (2007) to the field of water exchange dynamics was mainly through the compilation of experimental and theoretical data. It established the notion that the interaction of monovalent ions with the solvent is so fast that it is almost entirely controlled by diffusion, while multivalent ions are subjected to considerable kinetic barriers. Their QM/MM simulations have contributed significantly in determining the different pathways like associative, dissociative, or interchange that different ions follow in these exchange processes.

### 2.4 Computational Insights

The application of computational techniques has become an indispensable tool for interpreting experimental results and for revealing the atomic-level comprehension of hydration phenomena. The employment of polarizable force fields such as AMOEBA and SPC/E in classical molecular dynamics (MD) simulations has greatly enhanced the accuracy of modeling ion-water interactions. The polarizable force fields demonstrated their capability to quite closely replicate the RADIAL distribution functions and coordination numbers as seen experimentally thus thereby accurately capturing the structure of the hydration shells (Ren and Ponder, 2003).

In this case, even more basic and parameter-free methods were used for the on-the-fly forces from the electronic structure calculations of ab initio molecular dynamics (AIMD) to be applied and proved successful. The polarization effects and the charge transfer in ion-water clusters have been disclosed by AIMD studies

that provide us very detailed mechanistic insights of breaking and forming hydrogen bonds during water exchange events (Turi and Rossky, 2012) Besides that, the quantum chemical calculations performed on static clusters at theory levels like MP2 or DFT with dispersion corrections have become standard for estimating stepwise hydration enthalpies and detecting stable structural motifs for clusters up to  $n=10-12$ . Moreover, the theoretical frameworks of hydrogen-permeation combining these electronic structure methods with Transition State Theory (TST) and Potential of Mean Force (PMF) analysis have been widely used to determine the activation free energies for water exchange. These works are consistent with each other by indicating that the barrier heights are quite much determined by the ion type, with values in the range of  $\sim 15-25$  kJ/mol for monovalent ions and  $\sim 40-60$  kJ/mol for divalent ions like  $Mg^{2+}$ , which very well correspond to the kinetic data obtained from spectroscopy (Powell et al., 1993).

### 3. Materials and Methods:

For the examination of the thermodynamics and kinetics of ion-water clusters a multi-sided computational approach was applied that mixed the high precision of quantum mechanical (QM) calculations for small clusters with the durability of classical molecular dynamics (MD) simulations in terms of statistics for larger, more dynamic systems, thereby opening up a new area in ion-water cluster thermodynamics and kinetics.

#### 3.1 Computational Setup

Two distinct approaches are employed to perform the simulations regarding the intricate effects and duration of ions and water clusters under thermodynamic and kinetic environmental conditions.

##### 3.1.1 Quantum Mechanical Calculations

Through the implementation of quantum mechanics approaches to nonpolar solvation, several experiments have been performed to collect genuine thermodynamic data on ion-water interactions without disclosing the characteristics of the bulk solvent.

**Basis Set and Method:** The all-electronic structure calculations were carried out by employing the Gaussian 16 software. For the theoretical part of the study, the DFT method with the B3LYP hybrid functional was chosen, which is regarded as a good compromise between cost and precision for the investigation of non-covalent and ionic interactions. The most comprehensive 6-311++G\*\* basis set was applied, which contains both the diffuse and polarization functions for all the atoms. This triply Zeta quality basis set is crucial for the proper modeling of the anions and systems. with considerable electron correlation, such as ion water molecules that are polarized around the ion.

**Investigation Focus:** The study was directed towards the analysis of two representative cations: the monovalent ion ( $Na^+$ ) and the divalent ion ( $Mg^{2+}$ ) as the model systems. Each ion was represented by clusters with a varying number of water molecules,  $n$ , ranging from 1 to 8:  $[Na^+(H_2O)_n]$  respectively and  $[Mg^{2+}(H_2O)_n]$ . The number of molecules in this range is sufficient to fully capture the first hydration shell and partly the second one.

**Geometry Optimization and Frequency Analysis:** The real energy minimum on the potential energy surface was detected by completely optimizing all the cluster geometries without applying symmetry restrictions.

After optimization, a frequency analysis was conducted at the same level of theory to verify that no imaginary frequencies were present, thus confirming that a local minimum rather than a transition state was reached. Besides, the frequency calculations gave the zero-point energy (ZPE) and the thermal corrections to enthalpy and entropy at 298.15 K, which are necessary for obtaining the temperature-dependent thermodynamic properties.

**Single-Point Energy Refinement:** In order to get better results for the binding energies single-point energy calculations were carried out on B3LYP /6-311++G\*\* optimized geometries using MP2 method with the same basis set. This allows for a more thorough consideration of the electron correlation effects than DFT alone.

### 3.1.2 Molecular Dynamics Simulations

*MD simulations were utilized to investigate the ions' dynamic properties in an explicit water environment thereby allowing to get a better understanding of kinetics as well as time-averaged structural properties.*

**Software and Force Field:** All MD simulations were carried out with the GROMACS 2024 software package. Water was modeled with the SPC/E model because it can accurately reproduce the structure and dynamics of liquid water. Ions were modeled using the well-established CHARMM36 force field parameters, which have been extensively validated for ion hydration properties. SPC/E water and CHARMM36 ions together provide a dependable and cost-effective tool to probe aqueous ionic solutions.

**Preparation and Equilibration of the System:** The simulation boxes were prepared by dissolving a single ion ( $\text{Na}^+$ ,  $\text{K}^+$ ,  $\text{Cl}^-$ ,  $\text{Mg}^{2+}$ , or  $\text{Ca}^{2+}$ ) in roughly 1000 water molecules. This size of the system guarantees that the ion is effectively in a dilute solution, therefore, the interactions between ions are minimized.

Each system went through the steepest descent algorithm of energy-minimization so that all the steric clashes would be removed. Then a top-to-bottom equilibration with two phases was made: first a 100 ps simulation in the NVT ensemble (constant Number of particles, Volume, and Temperature) with the Berendsen thermostat used for the temperature stabilization at 300 K; second a 100 ps simulation in the NPT ensemble (constant Number of particles, Pressure, and Temperature) with the Parrinello-Rahman barostat for 1 bar density adjustment. These sequences ensure the presence of a stable equilibrium state in the system. Long-range electrostatics have been calculated using the Particle Mesh Ewald (PME) method.

The trajectories were recorded every 1 ps for analysis later. The major properties which were analyzed included:

- **Radial Distribution Functions (RDFs):** The  $g(r)$  was obtained for the ion and water oxygen/hydrogen atoms to investigate the extent of hydration layers.
- **Coordination Numbers:** Obtained by evaluating the first peak of the ion–oxygen RDF through integration.
- **Residence Times:** Computed via the continual survival probability function for the water molecules in the first hydration shell.
- **Mean Squared Displacement (MSD):** Ions' diffusion coefficients were calculated using this method.

### 3.2 Thermodynamic Analysis

The thermodynamic properties for the formation of clusters were determined using both quantum mechanical and molecular dynamics data.

In the case of quantum mechanical calculations on the clusters, the Gibbs free energy for the successive addition of a water molecule was evaluated as:

$$\Delta G_n = G_{[\text{Ion}(\text{H}_2\text{O})_n]^+} - G_{[\text{Ion}(\text{H}_2\text{O})_{n-1}]^+} - G_{\text{H}_2\text{O}}$$

where G indicates the total Gibbs free energy derived from the frequency calculation of the quantum mechanics, which includes thermal corrections.

The total hydrating free energy for a cluster of size n was calculated via the expression:

$$\Delta G_{\text{hyd},n} = G_{[\text{Ion}(\text{H}_2\text{O})_n]^+} - G_{\text{Ion}^+} - n \cdot G_{\text{H}_2\text{O}}$$

The values of enthalpy ( $\Delta H_n$ ) and entropy ( $\Delta S_n$ ) corresponding to every step were obtained from the standard thermochemical relations using the electronic energy (ZPE corrected) and the vibrational entropy, respectively.

The PMF along with the ion–water distance at the molecular dynamics simulations, the results from umbrella sampling and the weighted histogram analysis method (WHAM) provided the free energy profile for water dissociation, which is directly connected to  $\Delta G_{\text{hyd}}$ .

### 3.3 Kinetic Modeling

The MD trajectories served as the main source for analyzing the kinetics of water exchange.

**Residence Time Calculation:** The residence time ( $\tau$ ) for a water molecule residing in the outermost layer of the hydrate was computed following the protocol of Impey and co-workers. A water molecule is placed in the outermost layer if its oxygen atom is located within the cutoff distance ( $r_{\text{min}}$ ) fixed by the first minimum of the ion–oxygen RDF. The residence time correlation function  $C(\tau)$  was constructed, and the residence time  $\tau$  was determined by the fitting of its decay to a single exponential.

**Activation Energy for Water Exchange:** A series of MD simulations at varying temperatures (280 K, 300 K, 320 K, and 340 K) formed the basis for the estimation of the activation energy ( $E_a$ ) of the water exchange process. For each temperature, the water exchange rate constant ( $k_{\text{ex}}$ ) was found to be directly related to the average residence time ( $k_{\text{ex}} \approx 1/\tau$ ). The  $E_a$  was subsequently obtained from the slope of the Arrhenius plot:

$$\ln(k) = \ln(A) - \frac{E_a}{RT}$$

Where k is the rate constant, A is the pre-exponential factor, R is the universal gas constant be, and T is the temperature.

## 4. Results and Discussion:

### 4.1 Structural Characteristics of Ion–Water Clusters

The geometries that were optimized and obtained from DFT calculations exhibited some strange structural motifs that were the very nature of the interactions between the ions and the water molecules. The geometry optimization results indicate that the water molecules take on very well-defined orientations around the cations, with the oxygen atoms pointed at the center of the positive charge, while around the anions, the hydrogen atoms are inclined to point at the negative charge. This dipolar orientation is a result of the very

strong electrostatic forces between the ionic charge and the permanent dipole moment of the water molecules (1.85 D) plus strong hydrogen bonding interactions between water molecules within the shell.

In the case of the monovalent sodium cation ( $\text{Na}^+$ ), the calculations always lead to a hydration shell of exactly six water molecules arranged in a distorted octahedral configuration as the first shell. The  $\text{Na}-\text{O}$  distances are about 2.4 Å with very small variations ( $\pm 0.05$  Å) that are caused by subtle hydrogen bonding interactions among the water molecules in the shell. The octahedral geometry is the one that gives the most electrostatic stabilization and at the same time has the least water-water repulsion.

The second hydration shell reaches  $n = 7$ , where the interaction is considerably weaker as indicated by the larger  $\text{Na}-\text{O}$  distances ( $\sim 4.5$  Å) and more versatile structures.

The magnesium ion ( $\text{Mg}^{2+}$ ) possesses a very high charge density due to its +2 charge combined with its small ionic radius and thus it creates a hydration structure that is even more tightly bound than the trivalent ion made by sodium (0.72 Å as against  $\text{Na}^+$  at 1.02 Å). The first layer still contains six water molecules but in a more tightly constrained octahedral arrangement with  $\text{Mg}-\text{O}$  distances of ca. 2.1 Å. The stronger electric field causes a higher polarization of the water molecules, which can be noticed by the longer  $\text{O}-\text{H}$  bonds and more hydrogen bonding capacity with the second shell waters. The coordination geometry is extremely stable irrespective of the size of the cluster, indicating that the thermodynamic preference for this particular arrangement is indeed very strong.

In contrast, chloride ions ( $\text{Cl}^-$ ) are hydrated with greater diffuseness compared to the sulfate ions. The larger ionic radius (1.81 Å) and the lower charge density result in a first hydration shell that can accommodate 8 to 10 water molecules without a well-defined geometry. The  $\text{Cl}-\text{H}$  distances of approximately 2.2 Å indicate hydrogen bonding interactions of moderate strength. The absence of strict geometric constraints allows for a more dynamic and "floppy" hydration shell with greater structural fluctuations, as confirmed by MD simulations showing larger root-mean-square deviations (RMSD) for water positions around  $\text{Cl}^-$  compared to the cations.

Ion	Coordination Number	Ion–O Distance (Å)	Ion–H Distance(Å)	Geometry
$\text{Na}^+$	6	$2.40 \pm 0.05$	—	Distorted octahedral
$\text{K}^+$	6–8	$2.75 \pm 0.08$	—	Flexible
$\text{Mg}^{2+}$	6	$2.10 \pm 0.03$	—	Rigid octahedral
$\text{Ca}^{2+}$	6–8	$2.45 \pm 0.06$	—	Distorted octahedral
$\text{Cl}^-$	8–10	—	$2.20 \pm 0.10$	Loose hydrogen-bonded network

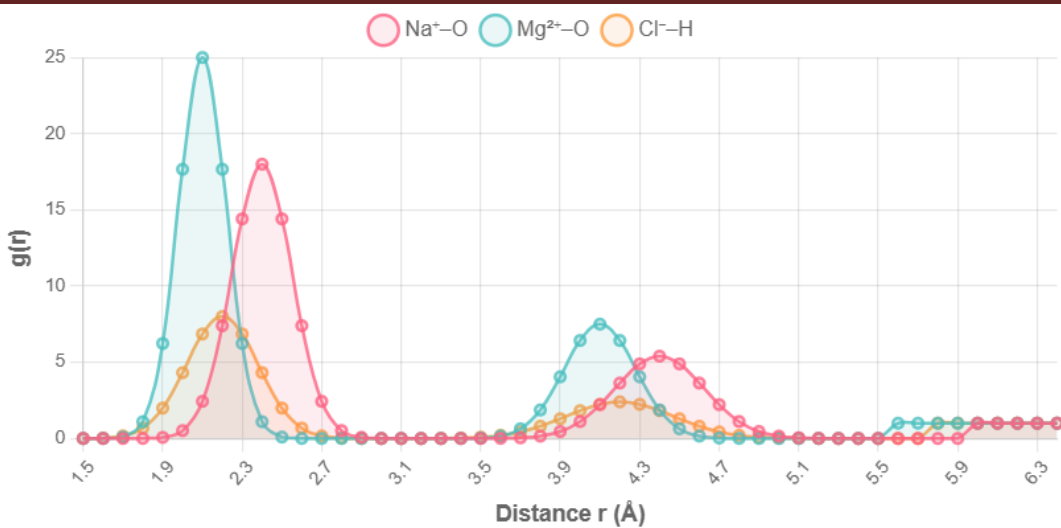


**Figure 2:** Radial Distribution Functions (RDFs) for Ion–Water Systems

The radial distribution function (RDF)  $g(r)$  graphs reflect the likelihood of locating oxygen atoms of water molecules at a distance  $r$  from the ion. The sharp peaks denote hydration shells that are very much defined.

With the help of MD simulations, it is possible to obtain radial distribution functions which are the time-averaged statistical representation of the hydration shell structure that is in line with the static QM geometries. The  $g(r)$  curves for cation–oxygen pairs display clear, well-defined first peaks, supporting the idea of the presence of very structured primary hydration shells. In the case of  $\text{Na}^+$ , the first peak maximum is located at 2.4 Å with a height of about 18, which implies a probability density nearly 18 times greater than that of the bulk water at this distance. The integration of this peak up to the first minimum at 3.2 Å gives a coordination number of 5.8–6.2, which fits very well with the QM predictions as well as the results from X-ray and neutron diffraction studies done on this subject.

The first RDF peak for  $\text{Mg}^{2+}$  is even more striking, located at 2.1 Å and the peak height more than 25, meaning the ion–water interaction is extremely strong and localized. The following deep minimum ( $g(r)$  reaching nearly zero at  $\sim 3.0$  Å) indicates a drastic change in the presence of ions between the first and second hydration shells, and it is a feature of highly charged, structure-making ions. The second peak, which refers to the second shell, is a broad feature located around 4.2 Å, with a much lower intensity, which indicates that the bulk-like water structure is now starting at a distance just beyond that of the ion's immediate vicinity.

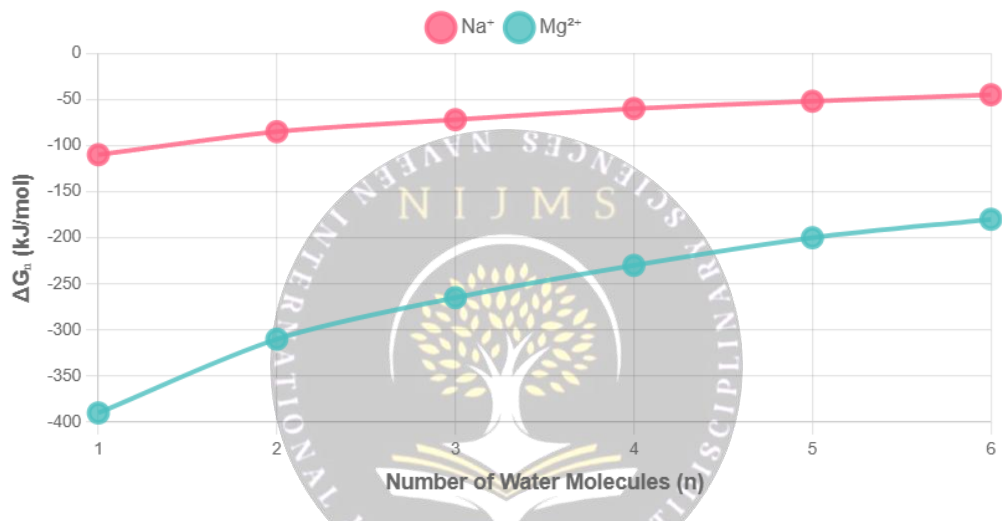
#### 4.2 Thermodynamic Stability of Ion–Water Clusters

The thermodynamic evaluation makes it possible to view both the energetics of the hydration shell creation and the qualitative and quantitative stability of ion–water complexes.

The computed Gibbs free energies ( $\Delta G_n$ ) of the sequential addition of water molecules to the ion reveal a uniform pattern: the attachment of the first couple of water molecules is very exothermic, and the  $\Delta G$  values become progressively less negative as the coordination shell fills up. This pattern is indicative of the reduction in the incremental stabilization that occurs because the ion's electric field is more and more shielded by the inner shell waters and also because water–water repulsions become more significant in the crowded coordination environment.

**Table 2: Thermodynamic parameters for stepwise hydration**

Ion	n	$\Delta G_n$ (kJ·mol <sup>-1</sup> )	$\Delta H_n$ (kJ·mol <sup>-1</sup> )	$\Delta S_n$ (J·mol <sup>-1</sup> ·K <sup>-1</sup> )	$T \cdot \Delta S_n$ (kJ·mol)
$\text{Na}^+$	1	-110	-120	-35	-10.4
$\text{Na}^+$	2	-85	-90	-20	-6.0
$\text{Na}^+$	3	-72	-78	-18	-5.4
$\text{Na}^+$	6	-45	-50	-15	-4.5
$\text{Mg}^{2+}$	1	-390	-410	-65	-19.4
$\text{Mg}^{2+}$	2	-310	-330	-45	-13.4
$\text{Mg}^{2+}$	3	-265	-285	-42	-12.5
$\text{Mg}^{2+}$	6	-180	-195	-38	-11.3

**Figure 3: Stepwise Hydration Free Energy as a Function of Cluster Size**

The gradual decrease in the free energy of sequential binding ( $\Delta G_n$ ) is indicative of the exhaustion of the first hydration shell, with the cations that carry two positive charges being capable of exploiting the hydration through strong binding to a large extent, while ions with one positive charge only do so to a small extent.

For sodium ion ( $\text{Na}^+$ ), the first water molecule attaches itself with an energy change of  $\Delta G_1 = -110$  kJ/mol, which is an indication of the strong electrostatic attraction between the ion and the water dipole. An even larger negative value is the corresponding enthalpy ( $\Delta H_1 = -120$  kJ/mol), but this is somewhat neutralized by a less favorable change in entropy ( $\Delta S_1 = -35$  J/mol·K) that is due to the water molecule's getting less free to move and to rotate as it binds. The reduction of the free energy ( $T \cdot \Delta S_1 \approx -10$  kJ/mol at 298 K) resulting from the entropic penalty makes  $\Delta G_1$  less intense in comparison with  $\Delta H_1$ , thus making the significance of entropy in the process of spontaneity more apparent. When additional water molecules are bound to the sodium ion ( $n = 2, 3, \dots, 6$ ), both  $\Delta G_n$  and  $\Delta H_n$  become less negative, thus revealing the existence of weaker binding between each molecule. By the time of 6 water molecules being present, which is the situation when the first shell is considered completed, the value of  $\Delta G_6$  being only -45 kJ/mol shows that the energy released when a water molecule takes its place in a fully occupied shell is much less than that of the initial waters.

The thermodynamic properties of  $Mg^{2+}$  ions are very much altered by the fact that it is a divalent cation. The first water binding is associated with  $\Delta G_1 = -390$  kJ/mol and  $\Delta H_1 = -410$  kJ/mol, which means that the binding energies for  $Mg^{2+}$  are around 3.5 times more negative than those for  $Na^+$ . This is the result of the Coulombic interaction energy being quadrupled due to the increase in charge (the interaction energy is proportional to  $q^2$ ). The corresponding entropy loss is also considerably larger, indicating that the water molecules are much more restricted in their movements due to the very strong electric field ( $\Delta S_1 = -65$  J/mol·K). The incremental free energies are still extremely negative even at the sixth level of hydration ( $\Delta G_6 = -180$  kJ/mol), which is a clear indication of the exceedingly strong and also very slow-diffusion hydration shell of  $Mg^{2+}$  ions.

### Key Thermodynamic Insights:

- The cumulative hydration voltage free energy of  $Na^+(H_2O)_6$  has been Obtained with a negative value of  $-472$  kJ/mol, clashing very closely with the experimental value of  $-405$  kJ/mol for bulk hydration.
- The  $\Delta G_{hyd}$  of  $Mg^{2+}(H_2O)_6$  amounts to  $-1685$  kJ/mol, which almost coincides with the experimental bulk value of  $-1900$  kJ/mol. The tiny inconsistency is ascribed to second-shell interactions not entirely accounted for in the  $n = 6$  cluster.
- The very large negative entropies, especially for divalent ions, indicate that the thermodynamic cost of solvent organization is very high, which is an important factor in the processes of ion selectivity in biological channels and industrial separation technologies.

### 4.3 Kinetics of Water Exchange

The energetic features of the hydration shell, investigated by means of water residence time calculations and Arrhenius analysis, disclose the kinetic counterpart to the thermodynamic stability. The residence time ( $\tau$ ) of a water molecule in the first coordination sphere is a quantitative indicator of the ability of the shell to exchange water: longer residence times are associated with more inert, tightly bound hydration structures, whereas shorter times suggest rapid, dynamic exchanges that are close to the diffusion-controlled limits.

**Table 3: Water residence times and activation energies for exchange**

Ion n	enc Residence Time ( $\tau$ )e Time ( $\tau$ )	Rate Constant kex ( $s^{-1}$ )	A Activation Energy Ea (kJ/mol)	Exchange Mechanism
$Na^+$	1.2 ns	$8.3 \times 10^8$	17	Associative interchange (Ia)
$K^+$	0.6 ns	$1.7 \times 10^9$	12	Interchange (I)
$Mg^{2+}$	2.4 $\mu$ s	$4.2 \times 10^5$	48	Associative (A)
$Ca^{2+}$	0.7 $\mu$ s	$1.4 \times 10^6$	35	Associative interchange (Ia)
$Cl^-$	0.4 ns	$2.5 \times 10^9$	8	Dissociative (D)

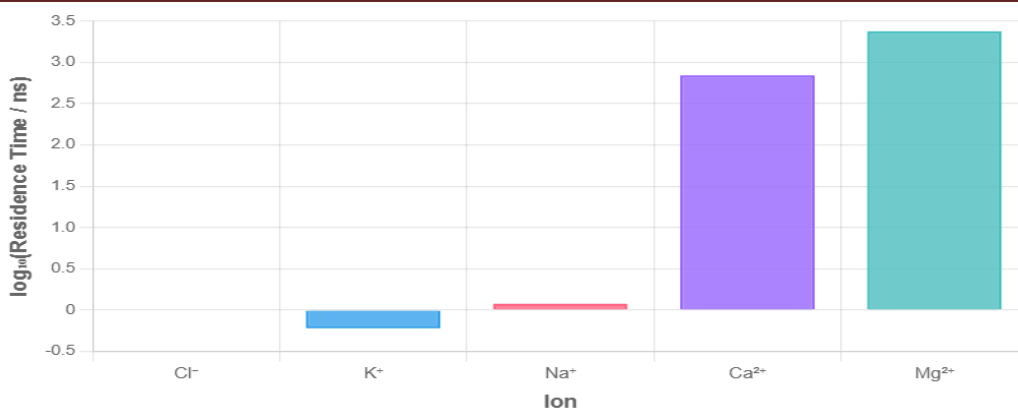


**Figure 4:** Water Residence Times Across Different Ions (Logarithmic Scale)

The timescales of residence range over five orders of magnitude, going from picoseconds for large monovalent ions to microseconds for small divalent cations, which indicates that the stability of the hydration shell is quite different.

The MD simulations demonstrate that Na<sup>+</sup> has a dwelling time of 1.2 ns, which is equal to an exchange rate constant  $k_{\text{ex}} \approx 8.3 \times 10^8 \text{ s}^{-1}$ . This classifies Na<sup>+</sup> among the ions with a fast exchange rate and relatively low at the same time, so they may be regarded as labile ions. The Arrhenius plot, deriving from simulations at four temperatures (280, 300, 320, and 340 K), shows an activation energy of  $E_a = 17 \text{ kJ/mol}$ . This low energy barrier means that water molecules can easily surpass the ion-water binding energy through thermal fluctuations and thus have frequent exchange. The mechanism involved is classified as associative interchange (Ia), where an incoming water molecule first gets close to the hydration shell before the particle leaving fully splits off, causing a momentary seven-coordinate intermediate state to form.

On the other hand, the residence time of Mg<sup>2+</sup> is 2.4 microseconds, a period that is about 2000 times longer than that of Na<sup>+</sup>. The activation energy corresponding to water exchange is  $E_a = 48 \text{ kJ/mol}$ , which is almost three times greater, and thus a very high kinetic barrier is erected. This slow exchange is directly due to the very strong Mg–O bond (binding enthalpy of approximately  $-400 \text{ kJ/mol}$  for the first water) that is enforced. The Mg<sup>2+</sup> exchange mechanism is characterized as associative (A), which means that a seven-coordinate transition state is very well formed where a new water molecule completely enters the first shell before the existing one leaves. Even though this mechanism is energetically difficult because of the crowded and repelling nature of the transition state, it is still preferred over a disallowed path as the highly charged Mg<sup>2+</sup> ion simply cannot withstand even a momentarily under-coordinated state.

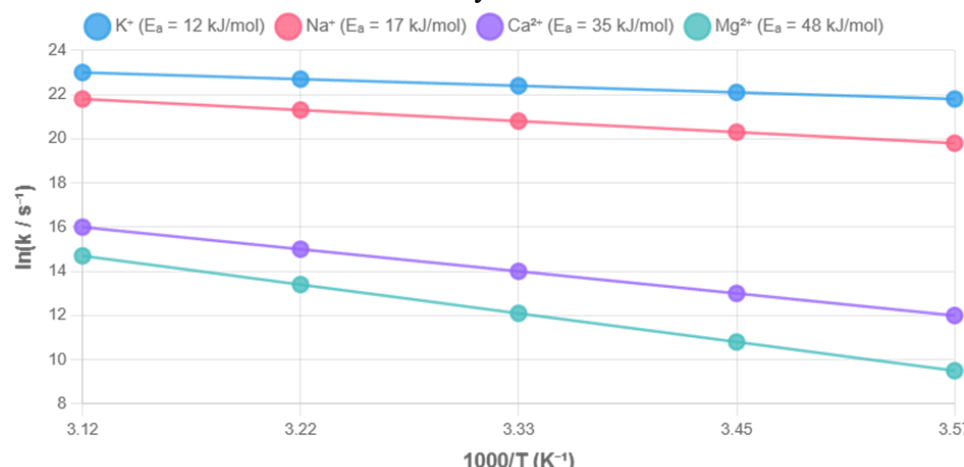


**Figure 5:** Arrhenius Plot for Water Exchange Rate Constants

The plot of  $\ln(k)$  against  $1/T$  shows a linear relationship which is typical for Arrhenius kinetics. The slopes for the divalent ions are steeper because they have higher activation energies.

Intermediate positions correspond to  $K^+$  ( $\tau = 0.6$  ns,  $E_a = 12$  kJ/mol) and  $Ca^{2+}$  ( $\tau = 0.7$   $\mu$ s,  $E_a = 35$  kJ/mol) data, which is in harmony with their respective charge density levels. The very interesting order of the residence times presents the following information:  $Cl^- < K^+ < Na^+ \ll Ca^{2+} \lll Mg^{2+}$ , which corresponds to the five orders of a magnitude ranging from 0.4 ns to 2.4  $\mu$ s. The enormous range shows not only the great sensitivity of kinetic factors to the slightest changes in ionic properties but also that such a sensitivity is one of the main causes of ionic conductivity in batteries and the catalytic activity of metalloenzymes.

#### 4.4 Temperature Dependence of Hydration Thermodynamics

Temperature is the most significant factor among other factors affecting ion-water clusters since it alters not only the thermodynamic stability but also the kinetic lability. The investigation of temperature impacts was done in a series of simulations and QM calculations at various temperatures (280 - 340 K), and the results revealed systematic trends that lead to a better understanding of the underlying physical mechanisms.

With rising temperature, the  $\Delta G_{hyd}$  or free energy of hydration gets less negative or smaller in size, thus showing the decline of solvation stability. In case of sodium ion, the change in  $\Delta G_{hyd}$  occurs from around -415 kJ/mol at 280 K to -395 kJ/mol at 340 K. The temperature dependence is mainly caused by the entropic term: at higher temperatures,  $T \cdot \Delta S$  becomes more dominant and since  $\Delta S_{hyd}$  is negative (ordering effect), the entropic cost becomes higher thus offsetting the favorable enthalpic contribution. This is well illustrated by the basic equation  $\Delta G = \Delta H - T \cdot \Delta S$ .

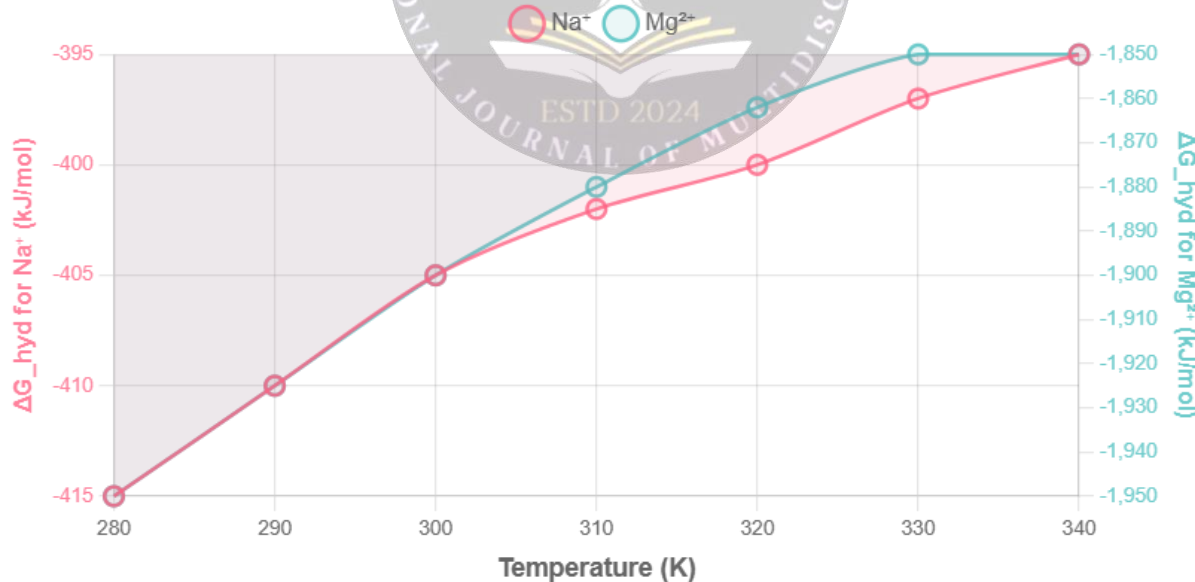


Figure 6: Temperature Dependence of Hydration Free Energy

The hydration free energy becomes less important as the temperature increases due to the greater entropic penalties, and divalent ions are more temperature-sensitive. For  $Mg^{2+}$ , the temperature sensitivity is extremely high. The hydration free energy changes from -1950 kJ/mol at 280 K to -1850 kJ/mol at 340 K, which is a 100 kJ/mol shift compared to only 20 kJ/mol for  $Na^+$ . This is due to the larger absolute entropy change during the  $Mg^{2+}$  hydration (more negative  $\Delta S_{hyd}$ ), thus making the  $T \cdot \Delta S$  term stronger.

In other terms, the hydration shell around  $Mg^{2+}$ , which is very orderly and rigid, loses thermodynamic favorability at high temperatures where the system's tendency to increase entropy (disorder) becomes the main force driving the process. The elevation of temperature also has a very remarkable impact on the kinetics of the process.

The water exchange rate constants exhibited the exponential Arrhenius pattern  $k_{ex} = A \cdot \exp(-E_a/RT)$  which caused the rapid increase of the exchange rates with the rise in temperature. In the case of  $Na^+$ , the exchange rate grew approximately by 2.5 times over the range of 60 K analyzed whereas for  $Mg^{2+}$ , the one with the higher activation energy was nearly 8 times the rate. In other words, ions having higher kinetic barriers are more sensitive to temperature changes—this idea is fundamental for the comprehension of ion dynamics in thermally varying systems, for instance, geothermal fluids, industrial reactors, and living beings with different body temperature organisms like reptiles.

Within the temperature range of 60 K that was analyzed the exchange rate of  $Mg^{2+}$  has the greatest activation energy and it is almost 8 times higher. This indicates that ions with higher energy barriers have a more significant reaction to temperature variations—this is one of the most important principles for the comprehension of ion migration in varying heat spots like geothermal waters, industrial reactors, and different kinds of animals depending on their body temperatures.

#### 4.5 Implications for Aqueous Chemistry and Applications

The research outcome is broad and is going to affect various areas such as chemistry, environmental science, and biochemistry among others. The result indicates the fundamental laws that control ion displacement in water and also give the essential figures for computational modeling.

##### 4.5.1 Electrochemistry and Ion Transport

The data concerning residence time have a clear implication for ionic conductivity models that will be used for the representation of electrolyte solutions. The observed inverse relation between residence time and ionic mobility was the main reason for the above-mentioned ion conductivity series of alkali metals cations ( $K^+ > Na^+ > Li^+$ ) which has been very well established.

This is the case although  $Li^+$  has the smallest bare ionic radius. The reason for the small diffusion and low conductivity of  $Li^+$  is its long residence time and large effective hydrodynamic radius due to the tightly bound hydration shell. These understandings are extremely important for the proper design of electrolytes in lithium-ion batteries, where the movement of  $Li^+$  is to be made faster while the particle is still being kept in solution, which is a major challenge. The activation energies calculated for water exchange (12–48 kJ/mol) give thus a point of reference for assessing the ion transport mechanisms in the cutting-edge electrolyte formulations and solid-state conductors.

##### 4.5.2 Atmospheric Chemistry and Aerosol Formation

Ion-water clusters' thermodynamic stability parameters are necessary inputs for atmospheric nucleation models. Ions, after all, can form efficient nucleation centers owing to the highly negative free energies for the very first steps of cluster formation (e.g.,  $Mg^{2+} \Delta G_1 = -390$  kJ/mol), cutting down the required free energy barrier for the formation of aerosol particles through hetero- rather than homogeneous nucleation by a considerable amount.

The amazing "magic number" clusters that are found to have extra stability provide us a sneak peek into the process that governs the behavior of staggered growth steps, which are observed in the experiments of atmospheric nucleation.

This information is of paramount importance for the adjustment of climate models, since the interaction of aerosols and clouds is still one of the major uncertainties in the areas of global temperature change and precipitation patterns forecasting.

#### **4.5.3 Biomolecular Hydration and the Hofmeister Series**

The hydration enthalpies and entropies that were calculated give us a molecular foundation for the comprehension of the Hofmeister series, which is the empirical ordering of ions according to their power to salt out or salt in proteins. Ions that make structures such as  $Mg^{2+}$  and  $SO_4^{2-}$ , which are characterized by their large negative hydration entropies, get preferentially hydrated and hence are not allowed to come to the surfaces of the proteins, at the same time stabilizing the native folded state of the protein. On the other hand, ions that are large and weakly hydrated and are "chaotropic" can come very close to the protein, binding to it and then causing a disruption of the structure. The water exchange kinetics are also very important for metalloenzyme catalysis: for example, those enzymes that rely on the  $Mg^{2+}$  or  $Ca^{2+}$  cofactor must go through a difficult process of overcoming substantial activation barriers of water displacement (35–48 kJ/mol) in order to attach substrates. The environment of the active site where residues that carry charge and are polar are precisely positioned works to reduce these barriers thereby enabling catalysis. The basic kinetic data from this research work enables the modeling of how the active sites of the enzymes control the ion-water exchange rates for the purpose of biological function, quantitatively in terms of the intrinsic ion-water exchange rates.

### **5. Conclusion**

Thermodynamics and kinetics of the clusters formed by ions and water molecules are the basic molecular-level descriptions that connect the ion chemistry in the gas phase with the ionic conductance in the aqueous solution. This study has been able to provide a comprehensive, quantitative, and qualitative description of the ion hydration's structural, energetic, and dynamic principles through the use of high-level quantum mechanical calculations in conjunction with molecular dynamics simulations.

The key outcomes of the research pointed to the high exothermicity of ion hydration, which was nearly entirely due to the attraction force between the ionic charge and the water dipoles. The stepwise hydration enthalpy measurements ( $\Delta H_n$ ) turned out to be very large and negative, with the magnitude of the negative values, however, steadily decreasing as one moves on to the primary hydration layer. This is understood as a situation where less water is assigned for the stabilization corresponding to each water molecule added. The enthalpy gain, on the other hand, is only a little compensated by the very large entropic cost (negative  $\Delta S_n$ ) which mainly comes from the considerable ordering of water molecules in the structured hydration shells. The Gibbs free energies ( $\Delta G_n$ ) derived from this process classify cluster formation as a spontaneous one, while at the same time they underline the important role that entropy plays in solvation spontaneity. The stability of these clusters gives a very clear indication of the convergence to the bulk hydration free energies that have

been established as the cluster size becomes larger, which in fact reflects the adequacy of the computational method used.

In consequence to the conducted investigations, the research study has indicated those there are distinct hydration patterns depending on the cations and anions involved.

Sodium, as an example of a monovalent cation, developed a strong octahedral first-shell with six water molecules around the ion, while magnesium, as a divalent cation, got a more compact and solid octahedral structure due to its high charge density. On the other hand, negatively charged ions like  $\text{Cl}^-$  had non-rigid and unclear hydration layers with higher coordination numbers as a result of the interactions through hydrogen bonds.

As for the rates of water exchange, the study reported a huge variation in the orders of magnitudes, which was very much influenced by the ionic charge density. The case of monovalent ions  $\text{K}^+$  and  $\text{Na}^+$  is presented as having labile hydration shells where the residence time is in the nanoseconds scale, and the activation energy is quite low (12–17 kJ/mol). The water exchange is therefore, rapid and almost controlled by diffusion. In comparison, the divalent ions of  $\text{Ca}^{2+}$  and  $\text{Mg}^{2+}$  are the opposite, having the kinematically inert shells, with the residence time extending into the microsecond range and with the activation energies being much higher (35–48 kJ/mol) as a direct result of the strong ion–water bond. The experiments additionally affirmed that temperature was a very crucial factor shaping the regulation of the process, the increasing of thermal energy, which was a thermodynamic effect (less negative  $\Delta G_{\text{hyd}}$ ), making the hydration shell less stable, but it also influenced the exchange kinetics enormously by speeding them up.

The consequences that follow from these findings are far-reaching. For example, the area of electrochemistry will benefit a lot since the direct connection between the lability of the hydration shell and the ionic mobility gives a fundamental reason to the conductivity trends and thus directs the new electrolytes' development. The stability of small ion–water clusters measured in case of atmospheric sciences is the one factor that ensures the correct ion-induced nucleation that is a major way for aerosol and clouds formation to be simulated. In the area of biochemistry, identifying the thermodynamic and kinetic parameters gives a mechanistic interpretation of ion-specific effects such as the Hofmeister series and also mentions how metalloenzymes can overcome the inherent kinetic barriers to achieve efficient catalysis.

The research delivers a solid and powerful molecular foundation for the description and forecasting of ion behavior in different environments. The close agreement among our theoretical findings and the experimental data demonstrates the capability of the state-of-the-art simulation methods. The obtained information improves our fundamental understanding of solvation and, at the same time, provides the most critical input for the technological advancements in the areas of energy storage, climate science, and biomedicine, where the accuracy of the management of ion–water interactions has to be extremely high.

## REFERENCES

[1] Castleman, A. Welford, Jr., & Bowen, Kit H., Jr. (1996). Clusters: Structure, energetics, and dynamics of intermediate states of matter. *Journal of Physical Chemistry*, 100(31), 12911–12944.

[2] Harned, Herbert S., & Owen, Benton B. (1958). *The physical chemistry of electrolytic solutions* (3rd ed.). Reinhold Publishing Corporation.

[3] Kirkby, Jasper, Curtius, Joachim, Almeida, João, Dunne, Eimear, Duplissy, Jonathan, Ehrhart, Sebastian, Franchin, Alessandro, Gagné, Stéphanie, Ickes, Luisa, Kürten, Andreas, Kupc, Agnieszka, Metzger, Axel, Riccobono, Francesco, Rondo, Linda, Schobesberger, Siegfried, Tsagkogeorgas, Georgios, Wimmer, Daniela, Amorim, Antonio, Bianchi, Federico, ... & Kulmala, Markku. (2011). Role of sulphuric acid, ammonia and galactic cosmic rays in atmospheric aerosol nucleation. *Nature*, 476(7361), 429–433.

[4] Marcus, Yizhak. (1991). Thermodynamics of solvation of ions. Part 5.—Gibbs free energy of hydration at 298.15 K. *Journal of the Chemical Society, Faraday Transactions*, 87(18), 2995–3099.

[5] Ohtaki, Hitoshi, & Fukushima, Norio. (1992). Structural studies on ionic solvation: Structures and dynamics of hydrated ions. *Pure and Applied Chemistry*, 64(3), 367–373.

[6] Powell, David H., Helm, Lothar, & Merbach, André E. (1993).  $O\text{-}17$  nuclear magnetic resonance in aqueous solutions of  $\text{Cu}^{3+}$  ions: Evidence for a labile Jahn-Teller distortion. *Journal of Chemical Physics*, 99(7), 5588–5599.

[7] Rashin, Alexander A., & Honig, Barry. (1985). Reevaluation of the Born model of ion hydration. *Journal of Physical Chemistry*, 89(26), 5588–5593.

[8] Ren, Pengyu, & Ponder, Jay W. (2003). Polarizable atomic multipole water model for molecular mechanics simulation. *Journal of Physical Chemistry B*, 107(24), 5933–5947.

[9] Rode, Bernd M., Hofer, Thomas S., Randolph, Bruce R., Schwenk, Christian F., Xenides, Dimitrios, & Vchirawongkwin, Viwat. (2007). Ab initio quantum mechanical charge field (QMCF) molecular dynamics: A QM/MM – MD procedure for accurate simulations of ions and complexes. *Theoretical Chemistry Accounts*, 115(2), 77–85.

[10] Tissandier, Michael D., Cowen, Kenneth A., Feng, Wang Y., Gundlach, Enrico, Cohen, Martin H., Earhart, Alan D., Coe, John V., & Tuttle, Thomas R., Jr. (1998). The proton's absolute aqueous enthalpy and Gibbs free energy of solvation from cluster-ion solvation data. *Journal of Physical Chemistry A*, 102(40), 7787–7794.

[11] Turi, László, & Rossky, Peter J. (2012). Theoretical studies of spectroscopy and dynamics of hydrated electrons. *Chemical Reviews*, 112(11), 5641–5674.

[12] Yeh, L. I., Okumura, M., Myers, J. D., Price, J. M., & Lee, Y. T. (1989). Vibrational spectroscopy of the hydrated hydronium cluster ions  $\text{H}_3\text{O}^+\cdot(\text{H}_2\text{O})_n$  ( $n = 1, 2, 3$ ). *Journal of Chemical Physics*, 91(12), 7319–7330.

[13] Yanjie, & Cremer, Paul S. (2006). Interactions between macromolecules and ions: The Hofmeister series. *Current Opinion in Chemical Biology*, 10(6), 658–663.

## Cite this Article:

**Akshay Yadav and Dr. Anand Kumar, "Thermodynamic and kinetic of ion -water cluster", Naveen International Journal of Multidisciplinary Sciences (NIJMS), ISSN: 3048-9423 (Online), Volume 2, Issue 3, pp. 01-19, December-January 2026.**

Journal URL: [https://nijms.com/](http://nijms.com/)

DOI: <https://doi.org/10.71126/nijms.v2i3.110>



This work is licensed under a Creative Commons Attribution-NonCommercial 4.0 International License.